AWARD NUMBER: W81XWH-16-1-0435

TITLE: Detection and Treatment of Advanced Prostate Cancer With Radiolabeled Transferrin Molecules

PRINCIPAL INVESTIGATOR: Dr. Ning Zhao

CONTRACTING ORGANIZATION: The Regents of the University of California, San Francisco
San Francisco, CA 94143-4249

REPORT DATE: SEPTEMBER 2017

TYPE OF REPORT: Annual

PREPARED FOR: U.S. Army Medical Research and Development Command
Fort Detrick, Maryland 21702-5012

REPORT DOCUMENTATION PAGE

Form Approved
OMB No. 0704-0188

1. REPORT DATE	2. REPORT TYPE	3. DATES COVERED
SEPTEMBER 2017	Annual	08/15/2016 – 08/14/2017

4. TITLE AND SUBTITLE

Detection and Treatment of Advanced Prostate Cancer With Radiolabeled Transferrin Molecules

5a. CONTRACT NUMBER
W81XWH-16-1-0435

5b. GRANT NUMBER

5c. PROGRAM ELEMENT NUMBER

6. AUTHORS

Dr. Ning Zhao

ning.zhao@ucsf.edu

5d. PROJECT NUMBER
0010830693

5e. TASK NUMBER

5f. WORK UNIT NUMBER

7. PERFORMING ORGANIZATION NAME(S) AND ADDRESS(ES)

The Regents of the University
of California, San Francisco
1855 Folsom St. Ste 425
San Francisco, CA 94143-4249

8. PERFORMING ORGANIZATION REPORT NUMBER

9. SPONSORING / MONITORING AGENCY NAME(S) AND ADDRESS(ES)

U.S. Army Medical Research and Development Command
Fort Detrick, Maryland 21702-5012

10. SPONSOR/MONITOR'S ACRONYM(S)

11. SPONSOR/MONITOR'S REPORT NUMBER(S)

12. DISTRIBUTION / AVAILABILITY STATEMENT

Approved for Public Release; Distribution Unlimited

13. SUPPLEMENTARY NOTES

14. ABSTRACT

We propose a new therapeutic paradigm for the treatment of castration resistant prostate cancer: targeting a shared pathobiological event upregulated by hyperactive MYC and mTOR with radiotherapy to ablate tumor cells. Because transferrin uptake into a cell is upregulated by hyperactive MYC or mTOR, we propose to synthesize a theranostic transferrin nanoparticle conjugate. A second objective is to show that we can image prostate cancer tumors with SPECT using the transferrin construct. The final objective is to show that the transferrin construct can ablate prostate cancer tumors with hyperactive MYC and/or mTOR.

15. SUBJECT TERMS

NONE LISTED

16. SECURITY CLASSIFICATION OF:			17. LIMITATION OF ABSTRACT	18. NUMBER OF PAGES	19a. NAME OF RESPONSIBLE PERSON
a. REPORT	b. ABSTRACT	c. THIS PAGE			USAMRMC
Unclassified	Unclassified	Unclassified	Unclassified	8	19b. TELEPHONE NUMBER *(include area code)*

TABLE OF CONTENTS

1. Introduction:

The central hypothesis of this proposal is that a Tf drug conjugate will induce cell death in castration resistant prostate cancer (CRPC) tumors because hyperactive MYC and mTOR are prevalent, and strongly upregulate transferrin (Tf) cellular uptake. Aim 1 focuses on the synthesis and in vitro characterization of ^{177}Lu-Tf-AGuIX, a nanoparticle construct for the treatment of CRPC. In Aim 2 focuses on the antitumor effects of ^{177}Lu-Tf-AGuIX in preclinical CRPC models harboring PTEN loss. Our novel approach has the potential redirect the community's effort away from moderately effective small molecule kinase inhibitors to ablative reagents that target downstream pathobiology regulated by mTOR. We feel Tf is a logical starting point to test the conceptual merit of this strategy, owing to its low cost, widespread availability, and clinical precedent showing on-target efficacy for Tf-drug conjugates in other indications with sporadic mTOR hyperactivation (melanoma, various glioma other than glioblastoma multiforme)[17,18]. Furthermore, AGuIX is a highly attractive nanoparticle platform to conjugate to Tf owing to the ease of its preparation (gram quantities can be synthesized in one GMP preparation), and a chemical versatility that allows for many orthogonal moieties to be appended to its polysiloxane core. Therefore, beyond the conceptual impact of introducing a new therapeutic paradigm for treating CRPC, we feel this proposal is exciting because the pathway to translation of ^{177}Lu-Tf-AGuIX is not hindered by many of the typical barriers associated with biomolecule-drug conjugates (e.g. the extreme cost of humanization and GMP production of the biomolecule). Lastly, the availability of a companion diagnostic in man (^{68}Ga-citrate imaging via PET) provides an important tool to establish the avidity of clinical TSC tumors for Tf well prior to the end of this funding period to stimulate enthusiasm for the translation of ^{177}Lu-Tf-AGuIX.

2. Keywords:

Iron, transferrin, nanoparticles, theranostics, lutetium-177, castration resistant prostate cancer.

3. Accomplishments:

In parallel with studies on the biodistribution of ^{177}Lu-TfAGuIX, we studied and reported the long term biodistribution of AGuIX in mice by labeling the nanoparticle (NP) with Zr-89. Below is a synopsis of the major findings, which we summarized for publication in *Molecular Pharmaceutics*:

AGuIX NPs were synthesized according to our previously established, top-down protocol. Briefly, gadolinium oxide cores were first synthesized in diethylene glycol. The oxide core was coated with a polysiloxane shell using hydrolysis–condensation of aminopropyl triethoxysilane (APTES) and tetraethyl orthosilicate (TEOS). DOTAGA groups (1,4,7,10-tetra-azacyclododecane-1-glutaric anhydride-4,7,10-triacetic acid) were then covalently ligated onto the nanoparticles via a primary amine from APTES. To induce core dissolution, the NPs were transferred from DEG to water. The resulting polysiloxane hollow cores were collapsed and fragmented into small and rigid platforms of polysiloxane. The resulting NPs bear on their surface DOTAGA molecules that are chelated to Gd^{3+} cations.[7]

To prepare DFO-AGuIX, 1-(4-isothiocyanatophenyl)-3- [6,17-dihydroxy-7,10,18,21-tetraoxo-27-(N-acetylhydroxylamino)-6,11,17,22-tetraazaheptaeicosine] thiourea (p-NCS-Bz-DFO) was incubated with AGuIX for one hour at room temperature. DFO was covalently ligated to the solvent exposed primary amines contained within APTES, and the resulting functional group was a thiourea. DFO-AGuIX was subjected to tangential filtration over a 5 kDa membrane to remove any unconjugated p-NCS-Bz-DFO at pH 5. . DFO-AGuIX NPs were then freeze−dried for storage. The freeze-dried nanoparticle is stable for months at low temperature.

We expected that adding DFO to AGuIX would change its retention on reverse phase HPLC. On this basis, we subjected DFO-AGuIX to RP-HPLC to determine its purity. Naked AGuIX, DFO-AGuIX, and free DFO were loaded into the injection loop separately. The corresponding chromatogram from the DFO-AGuIX showed peaks at 2.5 min corresponding to degradation fragments of DFO-AGuIX, while the principle peak at 13-14 min corresponds to DFO-AGuIX (**Figure 1A**). Moreover, DFO-AGuIX elutes later than AGuIX and no free DFO was detected in the DFO-AGuIX formulation. The final colloidal solution was characterized by dynamic light scattering and DFO-AGuIX was determined to have a hydrodynamic diameter of 4.4 ± 1 nm (slightly superior to the hydrodynamic diameter of naked AGuIX that is 3.6 ± 0.8 nm, **Figure 1B**), which is suitable for renal excretion.

A saturation binding assay was conducted with Cu^{2+} to determine the number of DFO chelators per AGuIX. Cu^{2+}ions in different proportions were added to DFO-AGuIX particles ([Gd^{3+}]= 38.4 mM). Using an absorbance filter of 700 nm, HPLC was applied to separate and detect free copper from chelated copper. A free fraction was initially detected at ~7 mM of Cu^{2+}, and This observation allowed us to estimate approximately one DFO chelator per DFO-AGuIX (**Figure 1C**). Notably, a separate set of experiments with Cu^{2+} and naked AGuIX showed almost no evidence of binding, indicating that the DOTAGA chelators within AGuIX are saturated with Gd^{3+} (free chelate < 2%), and the Cu^{2+} binding observed with DFO-AGuIX is due to an interaction between Cu^{2+} and DFO. Chemicals analysis performed on DFO-AGuIX are consistant with the following average composition: $Gd_1APTES^*_{2.78}TEOS^*_{2.66}DOTAGA^*_{1.02}DFO^*_{0.14}$ (see supplementary information). These results are in good agreement with the previous quantification of DFO per particle using Cu^{2+} complexation and separation by HPLC. DFO-AGuIX presents around 1 DFO chelator per particle.

DFO-AGuIX was metallated with ^{89}Zr-oxalate in one hour to a radiochemical yield of 99%. Unreacted ^{89}Zr-oxalate was removed by centrifugal membrane filtration. The radiochemical purity was 100% (**Figure 2A**).

We next evaluated the stability of ^{89}Zr-DFO-AGuIX *in vitro* and *in vivo*. No detectable degradation of ^{89}Zr-DFO-AGuIX was observed after 72 hours of incubation at 37^o C in bovine serum (**Figure 2B**). Moreover, no evidence of degradation was observed in the serum harvested from mice injected intravenously with ^{89}Zr-DFO-AGuIX (**Figure 2C**). Because ^{89}Zr-DFO-AGuIX was very stable, we determined the biological half-life of the construct in normal mice. Serial measurements of total activity in tumor naïve *nu/nu* mice injected with ^{89}Zr-AGuIX intravenously showed that the biological half-life is ~ 67 hours.

We next asked if ^{89}Zr-DFO-AGuIX accumulates within a subcutaneous tumor model in mice. Male *nu/nu* mice inoculated with subcutaneous U87MG tumors were injected with ^{89}Zr-DFO-AGuIX intravenously, and the biodistribution was monitored over time. After observing evidence of accumulation in the tumor with MRI 20 min post injection due to the positive contrast agent properties of DFO-AGuIX (r_1 = 16.7 $mmol^{-1}.s^{-1}$ and r_2/r_1 = 1.5 at 37°C and 1.4 T), we investigated the tumor associated activity from 24 – 72 hours with biodistribution studies. Durable retention of the NPs (~2% ID/g) was observed in human glioma U87MG tumors, and was statistically greater than the accumulation of ^{89}Zr-DFO (~0.5% ID/g at 24 hours post injection, see **Figure 3A** and **3B**). The tumor to blood and tumor to muscle ratio for ^{89}Zr-AGuIX incrementally increased over time to values greater than 10 at 72 hours post injection (**Figure 3C**). The uptake in other normal tissues was low, as expected, with the notable exception of the kidneys. Autoradiography of the tumor slices *ex vivo* also showed that the highest degree of activity within the tumor slices co-localized with areas harboring visually obvious pericellular compartments. Lastly, we tested whether ^{89}Zr-DFO-AGuIX was avid for peripheral mononuclear blood cells *in vivo*. After inducing an acute phase response with an intramuscular injection of turpentine, normal *nu/nu* mice were treated with ^{89}Zr—DFO-AGuIX or ^{89}Zr-transferrin, a molecule we previously showed to internalize into PMBCs. After 30 min, a biodistribution study was conducted to determine the amount of activity in the inflamed muscle and normal tissues. The uptake of ^{89}Zr-Tf was higher in the inflamed muscle compared to the untreated contralateral muscle, as expected. However, no difference in activity was observed between the inflamed and untreated muscles of mice treated with ^{89}Zr-AGuIX (**Figure 3D**). Moreover, the level of tissue associated activity in the inflamed muscle was ~0.5% ID/g, or roughly equal to what was observed for ^{89}Zr-DFO in U87MG tumors.

Figure 1. Synthesis and characterization of DFO-AGuIX. A. An overlay of reverse phase HPLC traces showing the resolution of DFO-AGuIX at ~15 min compared to naked AGuIX (~13 min) and free DFO (~16 min). These data also underscore the purity of DFO-AGuIX after filtration. B. DLS data showing that the hydrodynamic diameter of DFO-AGuIX is larger than naked AGuIX, as expected. These data were acquired using the purified DFO-AGuIX material. C. A Cu^{2+} saturation binding curve shows that AGuIX harbors about one DFO per nanoparticle. The area under the peak corresponding to free Cu^{2+} was calculated after addition of Cu^{2+} on DFO-AGuIX and injection in HPLC (See Supplemental Figure 1). Under sub-saturating conditions (1), no peak was detected, while increasing the concentration of Cu^{2+}, free Cu^{2+} ions were detected as the concentration exceeded ~7 mM (2). This assay was conducted with 38.4 mM AGuIX (in $[Gd^{3+}]$).

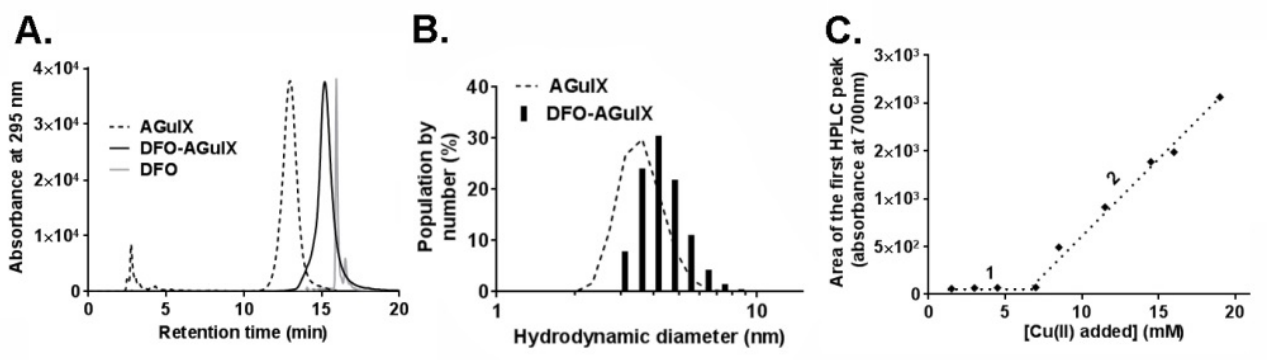

Figure 2. Synthesis and characterization of ^{89}Zr-DFO-AGuIX. A. A representative ITLC showing the near complete metallation of DFO-AGuIX with ^{89}Zr-oxalate. The large peak corresponds to activity at the baseline, interpreted to be ^{89}Zr-AGuIX, and an arrow indicates the expected R_f for ^{89}Zr-oxalate. B. Representative ITLC traces showing the stability of ^{89}Zr-DFO-AGuIX over time in neat fetal bovine serum. No peaks were resolved from baseline, suggesting that ^{89}Zr-DFO-AGuIX is not metabolized to smaller radioactive byproducts. C. Representative ITLC traces showing the stability of ^{89}Zr-DFO-AGuIX over time in in mouse serum. Mice were injected with ~50 □Ci of ^{89}Zr-DFO-AGuIX, and blood was harvested at the indicated time point.

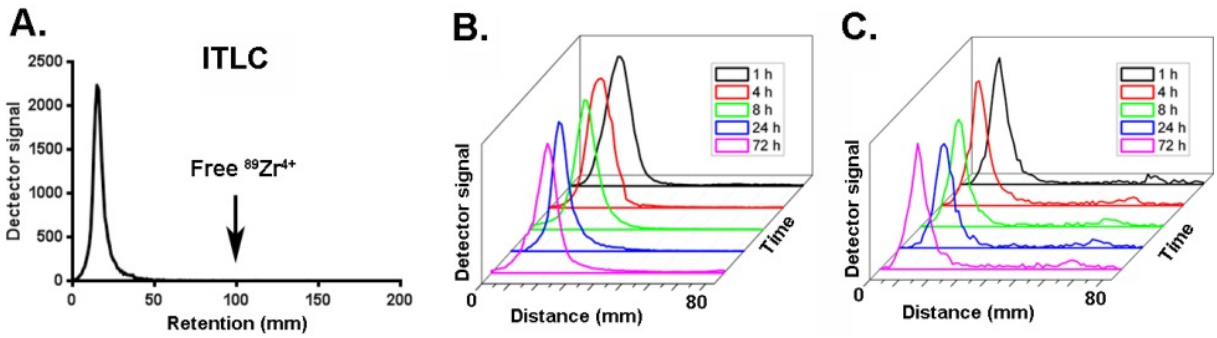

Figure 3. ^{89}Zr-DFO-AGuIX accumulates in the tumor microenvironment, but not in inflammatory abscesses. A. Biodistribution data at 24 hours post injection of ^{89}Zr-DFO-AGuIX or ^{89}Zr-DFO shows significantly higher uptake of the NP in the microenvironment of subcutaneous U87MG tumors compared to ^{89}Zr-DFO. No substantial differences were observed in muscle or bone, two normal reference tissues, from the cohorts receiving either radionuclide. B. Biodistribution data showing that ^{89}Zr-DFO-AGuIX persists in the tumor microenvironment for several days post injection. At 72 hours, the tumor associated activity was ~1.0% ID/g, which is above background. C. A graphical representation of the mean tumor to muscle and tumor to blood ratios over time for mice treated with ^{89}Zr-DFO-AGuIX. D. Biodistribution data showing no uptake of ^{89}Zr-DFO-AGuIX in the inflamed muscles within the hindlimbs of a mouse cohort. By comparison, ^{89}Zr-transferrin showed robust uptake in the inflamed muscle, owing to the abundant expression of the transferrin receptor on peripheral mononuclear blood cells. I.M. = inflamed muscle, C.M. = contralateral unmanipulated muscle.

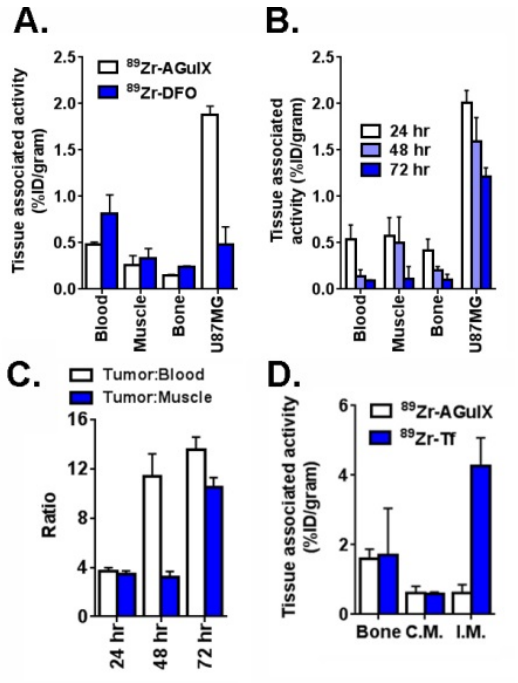

4. Impact

The data reported herein have significantly advanced the project by helping us to understand the biological half-life and biodistribution patterns of the NP in mice over time. Moreover, as we continue with antitumor assessment studies using ^{177}Lu-labeled forms of the NP, we note that enthusiasm for endoradiotherapies as a treatment for CRPC is increasing significantly. ^{177}Lu-PSMA 617 has entered clinical trials as a single agent therapy, and the early clinical data show that radiographic and biochemical responses occur for a majority of patients. Endoradiotherapies are also being explored as immunopriming agents for immunecheckpoint inhibitors. Thus, the deliverables from this project are timely and coincide with a growing movement toward developing endoradiotherapies for CRPC.

5. Changes/Problems

Nothing to Report.

6. Deliverables:

Truillet C, Thomas E, Lux F, Huynh LT, Tillement O, **Evans MJ**. Synthesis and Characterization of (89)Zr-Labeled Ultrasmall Nanoparticles. Mol Pharm. 2016 07 05; 13(7):2596-601. PMID: 27266800.

Lux F, Tran VL, Thomas E, Dufort S, Rossetti F, Martini M, **Truillet C**, Doussineau T, Bort G, Denat F, Boschetti F, Angelovski G, Detappe A, Crémillieux Y, Mignet N, Doan BT, Larrat B, Meriaux S, Barbier E, Roux S, Fries P, Müller A, Abadjian MC, Anderson C, Canet-Soulas E, Bouziotis P, Barberi-Heyob M, Frochot C, Verry C, Balosso J, **Evans M**, Sidi-Boumedine J, Janier M, Butterworth K, McMahon S, Prise K, Aloy MT,

Ardail D, Rodriguez-Lafrasse C, Porcel E, Lacombe S, Berbeco R, Allouch A, Perfettini JL, Chargari C, Deutsch E, Le Duc G, Tillement O. AGuIX® from bench to bedside-Transfer of an ultrasmall theranostic gadolinium-based nanoparticle to clinical medicine. Br J Radiol. 2018 Sep 18; 20180365. PMID: 30226413.

7. Participants and other collaborating organizations:

Nothing to report

8. Special reporting requirements

Nothing to report